

ORIGINAL  
ARTICLE

## Superoxide-dependent uptake of vitamin C in human glioma cells

Federico S. Rodríguez,\* Katterine A. Salazar,\* Nery A. Jara,\*  
María A. García-Robles,† Fernando Pérez,‡ Luciano E. Ferrada,\*  
Fernando Martínez\*† and Francisco J. Nualart\*\*Laboratory of Neurobiology and Stem Cells, Center for Advanced Microscopy CMA BIOBIO,  
University of Concepcion, Concepcion, Chile

†Laboratory of Cellular Biology, University of Concepcion, Concepcion, Chile

‡Hospital Guillermo Grant Benavente, Concepción, Chile

## Abstract

Glioblastomas are lethal brain tumors that resist current cytostatic therapies. Vitamin C may antagonize the effects of reactive oxygen species (ROS) generating therapies; however, it is often used to reduce therapy-related side effects despite its effects on therapy or tumor growth. Because the mechanisms of vitamin C uptake in gliomas are currently unknown, we evaluated the expression of the sodium-vitamin C cotransporter (SVCT) and facilitative hexose transporter (GLUT) families in human glioma cells. In addition, as microglial cells can greatly infiltrate high-grade gliomas (constituting up to 45% of cells in glioblastomas), the effect of TC620 glioma cell interactions with microglial-like HL60 cells on vitamin C uptake (Bystander effect) was determined. Although glioma cells expressed high levels of the SVCT

isoform-2 (SVCT2), low functional activity, intracellular localization and the expression of the dominant-negative isoform (dnSVCT2) were observed. The increased glucose metabolic activity of glioma cells was evident by the high 2-Deoxy-D-glucose and dehydroascorbic acid (DHA) uptake rates through the GLUT isoform-1 (GLUT1), the main DHA transporter in glioblastoma. Co-culture of glioma cells and activated microglial-like HL60 cells resulted in extracellular ascorbic acid oxidation and high DHA uptake by glioma cells. This Bystander effect may explain the high antioxidative potential observed in high-grade gliomas.

**Keywords:** glioblastoma, GLUT, microglia, SVCT2, vitamin C.

*J. Neurochem.* (2013) **127**, 793–804.

Gliomas are lethal tumors that occur in the CNS. The World Health Organization (WHO) classified gliomas into four histological categories; grades III and IV correspond to malignant gliomas (Louis *et al.* 2007). Glioblastoma multiforme (GBM, WHO grade IV) accounts for 50% of all intracranial tumors and 70% of primary malignant brain tumors (Wen and Kesari 2008). Although GBM often occurs in late adulthood (70% at a mean age of 53 years), up to 8.8% occur in children (Dohrmann *et al.* 1976; Ohgaki and Kleihues 2005). Because of the absence of specific symptoms, tumors are often detected at advanced stages, leading to poor prognosis with a mean survival of 1 year for GBM (Wen and Kesari 2008). Clinical trials using directed therapeutics, including bevacizumab, an angiogenesis inhibitor that targets vascular endothelial growth factor, have reported limited efficacy because of the adaptive nature of cancer cells (Watkins and Sontheimer 2012).

Reports have shown that vitamin C, a general antioxidant that is concentrated in the CNS, could impact tumor growth (Cameron and Pauling 1976; Heaney *et al.* 2008; Telang

Received May 6, 2013; revised manuscript received June 25, 2013; accepted July 8, 2013.

Address correspondence and reprint requests to Francisco Nualart, Departamento de Biología Celular, Facultad de Ciencias Biológicas, Casilla 160-C, Universidad de Concepción, Concepción, Chile. E-mail: fnualart@udec.cl

**Abbreviations used:** 2-DOG, 2-deoxy-D-glucose; AA, ascorbic acid; CLNX, calnexin; CNS, central nervous system; Cyt.B, zytochalasin B; DHA, dehydroascorbic acid; dnSVCT2, dominant-negative SVCT2; DPI, diphenyleioidonium; GBF-1, golgi-specific brefeldin A-resistance guanine nucleotide exchange factor-1; GBM, glioblastoma multiforme; GFAP, glial fibrillary acid protein; GLUT, facilitative hexose transporter; IC<sub>50</sub>, half maximal inhibitory concentration; Km, michaelis constant; NBT, nitroblue tetrazolium; ROS, reactive oxygen species; SVCT2, sodium-vitamin C co-transporter isoform 2; UIB, uptake incubation buffer; Vmax, maximum velocity; WHO, world health organization.

*et al.* 2007). Although more than three decades ago Linus Pauling and Ewan Cameron proposed the benefits of megadose vitamin C treatment for patients with advanced cancer (Cameron and Pauling 1976, 1978), reproducible effects have been lacking (Moertel *et al.* 1985). It is likely that some of the conflicting data arose from incomplete knowledge of vitamin C physiology and uptake mechanisms. Vitamin C exists in two redox states: (i) ascorbic acid (AA), which is the most stable and abundant form, and (ii) dehydroascorbic acid (DHA), which is present at low levels (<5%) and can be rapidly recycled to AA in the blood and brain (Astuya *et al.* 2005; Mendiratta *et al.* 1998; Rice 2000). Two transporter families mediate cellular uptake of vitamin C in the CNS. The sodium vitamin C co-transporter isoform 2 (SVCT2) mediates concentrative AA uptake (Liang *et al.* 2001). In addition, some of the 14 isoforms of the facilitative hexose transporter (GLUT) family mediate gradient-directed uptake of DHA (Nualart *et al.* 2003; Rumsey *et al.* 1997).

Peripheral tumors, including leukemia, as well as breast and prostate cancer cell lines are incapable of accumulating vitamin C through SVCT2 (Guaiquil *et al.* 1997; Nualart *et al.* 2003). However, we have previously described a mechanism that could allow massive DHA uptake into tumor cells, termed the Bystander effect (Nualart *et al.* 2003). This mechanism involves infiltration of the tumor by superoxide-releasing neutrophils, generating stromal oxidation of AA to DHA and DHA uptake by nearby tumor cells through GLUT1, GLUT3, or GLUT4 (Rumsey *et al.* 1997). To accumulate intracellularly, DHA must be compartmentalized or reduced by enzymatic or non-enzymatic mechanisms (Linster and Van Schaftingen 2007).

Gliomas contain an increasing proportion of microglial cells with malignancy (Yi *et al.* 2011), resulting in enhanced tumor growth (Zhai *et al.* 2011). For example, microglia can account for up to 45% of the cell population in GBM (Morantz *et al.* 1979; Nishie *et al.* 1999; Seyfried 2001; Shinonaga *et al.* 1988). Because of the close association between microglia and glioma cells coupled with superoxide generation by microglia (Sankarapandi *et al.* 1998), this study tested the hypothesis that increased vitamin C uptake through the Bystander effect induces increased antioxidative capacity in gliomas that may mediate their resistance to therapies. The mechanisms of vitamin C uptake in glioma cells with histological correlation to glioma biology were evaluated. Analysis of vitamin C transporter expression and function in human glioma cells *in vitro* was undertaken. However, glioma cells uptake very low levels of AA, their high capacity for DHA uptake could generate massive cellular loads of AA through GLUT1-mediated DHA transport. A detailed description of vitamin C uptake by glioma cells may yield novel therapeutic targets for patients with malignant gliomas.

## Materials and methods

### Cell cultures

TC620 (Manuelidis *et al.* 1977; Astuya *et al.* 2005), U87MG (ATCC, Manassas, VA, USA) and HL60 cells (Nualart *et al.* 2003) were grown in Iscove's Modified Dulbecco's Medium (Sigma Life Science, St. Louis, MO, USA) supplemented with 10% fetal bovine serum (Hyclone Laboratories, Inc., Logan, UT, USA), 2 mM glutamine, 100 U/mL penicillin, 100 µg/mL streptomycin (Gibco, Invitrogen, Grand Island, NY, USA), and 250 pg/mL fungizone (Hyclone Laboratories, Inc.). AA was not detected in the culture medium by HPLC method.

Primary glioma cultures were obtained from surgically resected human astrocytomas (WHO grades III and IV) from two male patients in accordance with the accepted standards of the ethics committee on the use of human specimens at UCO 2013101H and after informed consent was obtained from both patients. Tissues were rapidly cut in pieces less than 1 mm in size, rinsed in 0.1 M phosphate buffer (pH 7.4, 320 mOsm), incubated for 10 min in 0.25% trypsin, and dissociated mechanically to homogeneity with a fire-polished Pasteur pipette. Cells were then seeded at low-density ( $2 \times 10^3$  cells/cm<sup>2</sup>) in 100-mm dishes (BD Corning™, Franklin lanes, NJ, USA), and maintained in Dulbecco's modified Eagle's medium/F12 (Sigma Life Science) supplemented with 5% fetal bovine serum and antibiotics. Fresh medium was added every 2–3 days, and after 30 days, selected cell colonies from grade III (TC233) and IV (TC236) astrocytomas were harvested and plated ( $2 \times 10^5$  cells/cm<sup>2</sup>) for experimental analysis.

### Immunocytochemistry

Formalin-fixed and paraffin-embedded human GBM tissue sections (7 µm) were deparaffinized and rehydrated; endogenous peroxidase activity was inhibited with 3% H<sub>2</sub>O<sub>2</sub> dissolved in methanol (Nualart *et al.* 2012a). TC620 and U87 cells were cultured on 12-mm round coverslips for 24 h and fixed 30 min in 4% paraformaldehyde. HL60 cells were cultured on poly-L-lysine-coated coverslips after addition of 1 µM phorbol-12-myristate-13-acetate (PMA) for 24 h and processed for immunocytochemistry. Before incubation with the primary antibodies, cells were permeabilized by incubation in 0.02% triton X-100 phosphate buffer (pH 7.8) for 10 min. The following affinity-purified polyclonal primary antibodies were used: anti-GLUT1-GLUT5 (Alpha Diagnostic, San Antonio, TX, USA); anti-SVCT2 (G19, Santa Cruz Biotechnology Inc., Santa Cruz, CA, USA); anti-p47Phox (Upstate, Lake Placid, NY, USA); anti-Golgi-specific brefeldin-A resistance guanine nucleotide exchange factor-1 (GBF-1; kindly donated by Dr Alejandro Claude); anti-calnexin, anti-early endosome antigen-1 protein, and anti-mannose 6-phosphate receptor (M6PR) (all from Abcam Inc., Cambridge, MA, USA); and anti-gial fibrillary acid protein (GFAP) and anti-vimentin (Dako Inc., Glostrup, Denmark). After washing, tissue samples were incubated for 2 h at 22°C with secondary antibodies conjugated to horseradish peroxidase (Jackson ImmunoResearch Laboratories, Inc., West Grove, PA, USA), and labeling was performed with the 3,3-diaminobenzidine and H<sub>2</sub>O<sub>2</sub> reaction (Godoy *et al.* 2006). Cells on coverslips were incubated with secondary antibodies conjugated to fluorescent dyes (Jackson ImmunoResearch Laboratories Inc.), and DNA was stained using TOPRO-3 (1 : 1000; Invitrogen, Rockville, MD, USA) or propidium iodide (Molecular Probes Inc., Eugene, OR, USA). The cells were

analyzed by confocal laser microscopy (Carl Zeiss LSM 780, Jena, Germany).

#### RT-PCR analysis

Total RNA was extracted from cultured TC620 cells using TRIzol® reagent (Invitrogen, Carlsbad, CA, USA). Synthesis of cDNA and PCR were performed using standard procedures (Millan *et al.* 2010). The thermocycling conditions were as follows: 94°C for 5 min followed by 35 cycles of 94°C for 30 s, 55°C for 30–50 s, and 72°C for 30 s for 35 cycles; with a final extension of 7 min at 72°C. The following sets of primers were used: **β-actin**, SN-5'-GCTGCTCGTCGACAACGGCTC-3', AS-3'-CAAACATGATCTGGGTCATCTTCTC-5' (353 bp); **SVCT2a**, SN-5'-GAGGCAAA GCACCCAGCTTT-3', AS-5'- AACAGAGAGGCCAATTAGGG-3' (700 bp); **SVCT2b**, SN-5'-GGGGCTACAGCACTACCTG-3', AS-5'-AACAGAGAGGCCAATTAGGG-3' (461 bp); **SVCT2c**, SN-5'-TTCTGTGTGGGAATCACTAC-3', AS-5'-ACAGAGAGGCCAATTAGGG-3' (340 bp); **SVCT2d**, SN-5'-GGGGCTACAGCACTACCTG-3', AS-5'-GGATGGCCAGGATGATAG-3' (647 bp and 305 bp); **GLUT1** SN-5'-TGAACCTGCTGGCCTTC-3', AS-5'-GCAGCTTCTTTAGCACA-3' (399 bp); **GLUT2**, SN-5'-CAACAGGTAATAATATC-3', AS-5'-CTCGCACACCAGACAGG-3' (583 bp); **GLUT3**, SN-5'-AAGGATAACTATAATGG-3', AS-5'-GGTCTCCTTAGCAGGCT-3' (411 bp); **GLUT4**, SN-5'-CA GAAGGTGATTGAACA-3', AS-3'-CAGGTAGCACTGTGAGG-5' (493 bp); and **GLUT5**, SN-5'-GAATTCATGGAAGACTT-3', AS-5'-GCCATCTACGTTTGCAA-3' (396 bp).

#### Immunoblotting

For immunoblot analysis, total protein extracts isolated from the cytosol and membranes of  $5 \times 10^6$  U-87 cells, membrane enriched protein extracts from  $5 \times 10^7$  TC620 cells, and equivalent volumes of rat brain or dissected rat hypothalamus were obtained by homogenizing samples in 0.3 mM sucrose, 1 mM EDTA and a complete protease inhibitor cocktail (Roche, Indianapolis, IN, USA) as previously described (Garcia Mde *et al.* 2005). Proteins (50–100 µg) were resolved by 5–15% (w/v) gradient sodium dodecyl sulfate–polyacrylamide gel electrophoresis, electrotransferred to Immobilon®-P membranes (0.45 µm pore size; Millipore Corporation, Billerica, MA, USA) and probed overnight with anti-GLUT1, anti-GLUT3 (1 : 1000; Alpha Diagnostic), or anti-SVCT2 (1 : 200; Santa Cruz Biotechnology Inc.). After incubation with horseradish peroxidase-conjugated secondary antibodies (1 : 5000; Jackson ImmunoResearch), the reaction was developed with enhanced chemiluminescence reagent (Amersham Biosciences, Pittsburgh, PA, USA).

#### Uptake assays

For uptake assays, cells were grown in 6-well plates to a density of  $8 \times 10^5$  cells/well as previously described (Garcia *et al.* 2003). Briefly, cells were incubated in uptake incubation buffer consisting of 15 mM HEPES pH 7.0, 135 mM NaCl, 5 mM KCl, 1.8 mM CaCl<sub>2</sub>, 0.8 mM MgCl<sub>2</sub>, 320 mOsm (Nualart *et al.* 2003) for 10 min at 37°C for ion equilibration. Uptake was performed using 1 µCi 2-Deoxy-D-glucose (2-DOG; 26.2 Ci/mmol; Dupont NEN, Boston, MA, USA) or 5–100 µM 1-<sup>14</sup>C-L-AA (8.5 mCi/mmol, PerkinElmer Life Science, Boston, MA, USA) with 0.1 mM dithiothreitol for AA preservation. DHA was yielded by oxidizing AA with 5 U/µmol of

ascorbate oxidase (Sigma-Aldrich) (Nualart *et al.* 2003). Uptake was stopped using ice-cold uptake incubation buffer with 0.2 mM HgCl<sub>2</sub> and cells were homogenized in 400 µL of lysis buffer (10 mM Tris-HCl pH 8.0 and 0.2% sodium dodecyl sulfate). The incorporated radioactivity was measured by liquid scintillation spectrometry (Beckman Coulter LS 6500; Beckman Coulter, Inc., Brea CA, USA). Saturation assays were performed at the initial velocity range. Uptake of 2-DOG and DHA was performed at 22°C whereas AA uptake was performed at 37°C.

#### Detection of cellular superoxide production and liberation

Superoxide production was quantified by monitoring ferricytochrome C reduction (Sigma-Aldrich). Cells were suspended in modified Hepes Krebs Ringer buffer (20 mM Hepes, pH 7.4, 130 mM NaCl, 5 mM KCl, 1.2 mM MgSO<sub>4</sub>, 1.2 mM CaCl<sub>2</sub>, Na<sub>2</sub>HPO<sub>4</sub>, 1 mM D-glucose, 0.1% bovine serum albumin) containing 1 mg/mL ferricytochrome C and activated by the addition of 1 µM PMA. The reduction of ferricytochrome C was monitored by determining the change in the absorbance at 550 nm, and extracellular superoxide was calculated using an extinction coefficient of 21 000 M<sup>-1</sup> cm<sup>-1</sup> (Nualart *et al.* 2003). Intracellular oxidant generation was defined using the nitrobluetetrazolium (NBT) reduction technique (Sudo *et al.* 1998). PMA-activated HL60 cells were incubated 1 h with 0.5 mg/mL NBT in Hepes Krebs Ringer buffer. Intracellular blue formazan deposits were microscopically visualized after washing with 60% methanol and 4% paraformaldehyde fixation. Diphenylene iodonium (DPI), a NADPH-oxidase inhibitor, and temperature dependence were used as controls.

#### Statistical analysis

Data presented in this article are the results of three independent experiments performed in triplicates and expressed as means ± SD. Studies evaluating superoxide generation and uptake of 2-DOG, AA, and DHA were analyzed using Student's unpaired *t*-tests.

## Results

### Glioma cells have low capacity for AA uptake because of intracellular SVCT2 localization

Only few specialized glial cells, including tanycytes and choroid plexus cells, are capable of AA transport in the CNS (Angelow *et al.* 2003; Garcia Mde *et al.* 2005); however, the ability of glioma cells to uptake AA had not been previously assessed. Because SVCT2 was the only AA transporter reported in the adult CNS to date (Nualart *et al.* 2012b), the functional activity of SVCT2 was evaluated in cultured human glioma cells. Radiolabeled AA uptake in TC620 cells was extremely low at 5 min, reaching 40 pmol × 10<sup>6</sup> cells (Fig. 1a); however, it was sensitive to both temperature and sodium availability (Fig. 1b). In addition, the functional identity of SVCT2 was defined through kinetic parameters in dose-response assays. Uptake of 5–100 µM AA at 30 s resulted in a Michaelian curve with saturation at 60 µM AA (Fig. 1c), and the double reciprocal plot revealed a single functional component with a Michaelis constant ( $K_m$ ) of

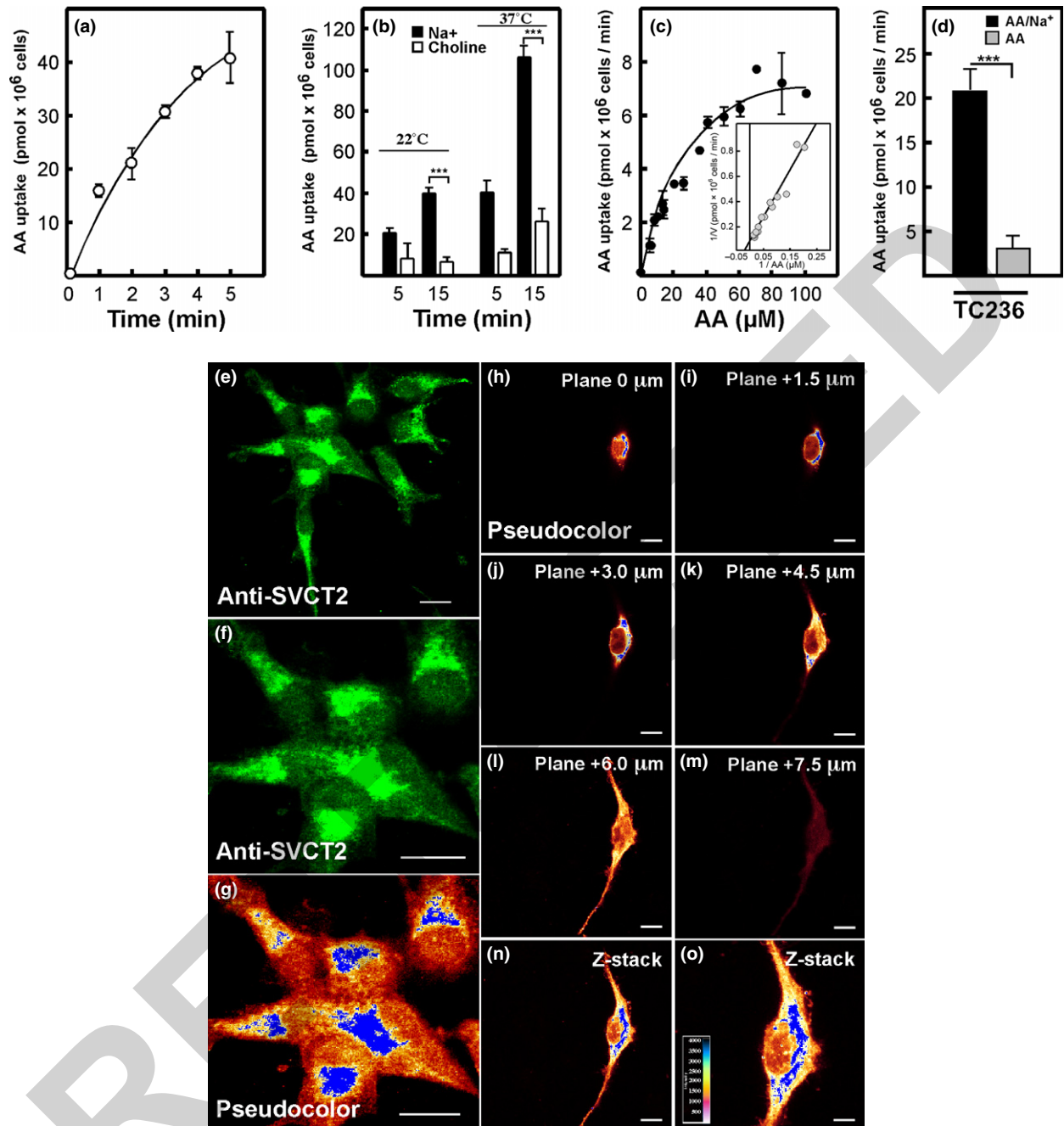


**Fig. 1** Ascorbic acid (AA) uptake and immunolocalization of sodium-vitamin C co-transporter isoform 2 (SVCT2) in glioma cells. (a) Time course of 100  $\mu\text{M}$  AA uptake. (b) Temperature- and sodium-dependent AA (100  $\mu\text{M}$ ) uptake. (c) Saturation plot using 5–100  $\mu\text{M}$  AA uptake at 30 s. Inset, Lineweaver–Burk plot of the data presented in (c). (d) AA uptake in cultures of human glioblastoma multiforme biopsies. (e–g)

Mid-plane confocal immunolocalization of SVCT2 (green) in TC620 cells. (h–o), Confocal 3D-rendering analysis showing pseudocolor (blue) for highest SVCT2 immunolocalization. Kinetic data were performed at 37°C unless indicated otherwise. Data represent means  $\pm$  SD of three independent experiments. \*\*\* $p > 0.001$ , Student's unpaired  $t$ -test. Scale bars, 25  $\mu\text{m}$ .

25  $\mu\text{M}$  and a maximum velocity ( $V_{\text{max}}$ ) of 7 pmol  $\times$  10<sup>6</sup> cells/min (Fig. 1c; inset) in accordance with a previous study (Savini *et al.* 2008). Similar uptake assays in human GBM cells (TC236) confirmed low AA uptake levels

(21 pmol  $\times$  10<sup>6</sup> cells/min) and sensitivity to sodium (Fig. 1d). To confirm SVCT2 expression, confocal immunocytochemical detection of SVCT2 was undertaken. Mid-plane confocal images showed high levels of SVCT2 in

glioma cells (Fig. 1e and f, green). However, the highest immunocytochemical detection as represented by pseudo-color (Fig. 1g; blue color) showed the intracellular localization of SVCT2. Moreover, whole cell 3D-rendering analysis (Fig. 1h–o) confirmed the intracellular localization of SVCT2 in all focal planes across the cell.

#### Glioma cells express the dominant-negative SVCT2 isoform

Previous reports have shown that intracellular localization of SVCT2 and low AA uptake can be induced by the expression of a dominant-negative isoform of SVCT2 termed, dominant-negative SVCT2 (dnSVCT2) (Lutsenko *et al.* 2004; Wu *et al.* 2007). To identify the possible cause of intracellular SVCT2 localization, the expression of the dnSVCT2 in TC620 cells was assessed. RT-PCR assays using specific primers for SVCT2 isoforms, with antisense primers annealing within the predicted splice sequence (Fig. 2a) showed the presence of a single amplification product of the correct size (Fig. 2a; lanes 1–3). However, primers flanking the predicted splice sequence amplified two PCR products with the predicted sizes corresponding to the full length and dnSVCT2 isoforms (Fig. 2a; lane 4). Western blot analyses of SVCT2 expression in membrane-enriched protein extracts from TC620 glioma cells, and positive control tissues from

rat hypothalamus and whole brain were also undertaken (Fig. 2b). Glioma samples showed three polypeptide bands of different molecular mass (Fig. 2b, lane 1). The fainter 75 kDa band co-migrated with hypothalamic and whole brain positive control tissues known to be functionally active in AA uptake (Fig. 2b; lanes 2–3). Two additional bands of approximately 50 kDa and 130 kDa, which were not detected in the absence of the primary antibody, were observed in the glioma samples (Fig. 2b, lanes 4–6). In addition, the co-localization of SVCT2 with subcellular organelles was assessed using markers for Golgi apparatus, endoplasmic reticulum, early- and late-endosomes. The highest co-localization was observed with Golgi (GBF1) and endoplasmic reticulum (calnexin) markers (Fig. 2c, d and g, h), while no relevant co-localization was observed with endosomes (Fig. 2e, f and i, j).

The *in vitro* localization experiments were confirmed using human GBM biopsies (Fig. 3). GBM tumor cells were identified by anti-vimentin and anti-GFAP immunostaining and cell morphology as described previously (Schiffer *et al.* 2006). Representative bright-field microscopy images revealed extensive vimentin and GFAP expression in cells with typical gemistocytic and rhabdoid morphology (Fig. 3a–f). Immunocytochemical analysis for SVCT2

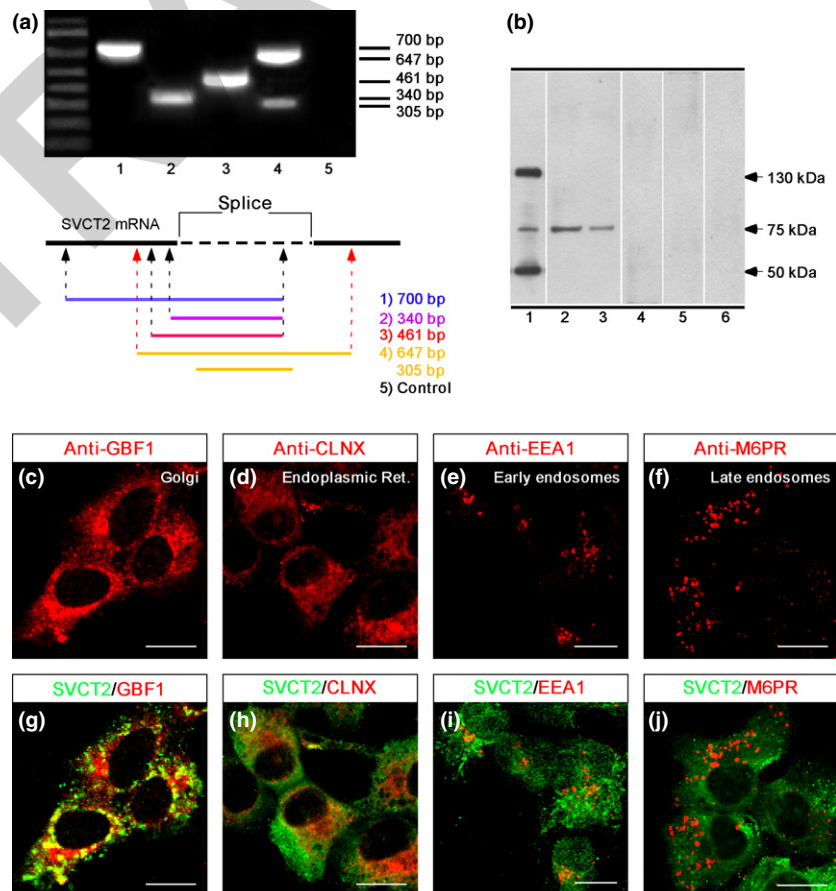


**Fig. 2** Molecular analysis of sodium-vitamin C co-transporter isoform 2 (SVCT2) expression in cultured TC620 cells. (a) RT-PCR analysis using specific primers for SVCT2 amplification as shown in diagram (below). (b) Western blot analysis for SVCT2 using membrane protein extracts of TC620 cells (lane 1), rat hypothalamus (lane 2), and whole rat brain (lane 3). Lanes 4–6 represent control reactions without primary antibody. (c–f) Immunolocalization of subcellular organelles in cultured TC620 cells. (g–j) Co-localization of SVCT2 immunoreactivity with subcellular organelle markers shown in the upper panels. Scale bars, 20  $\mu$ m.

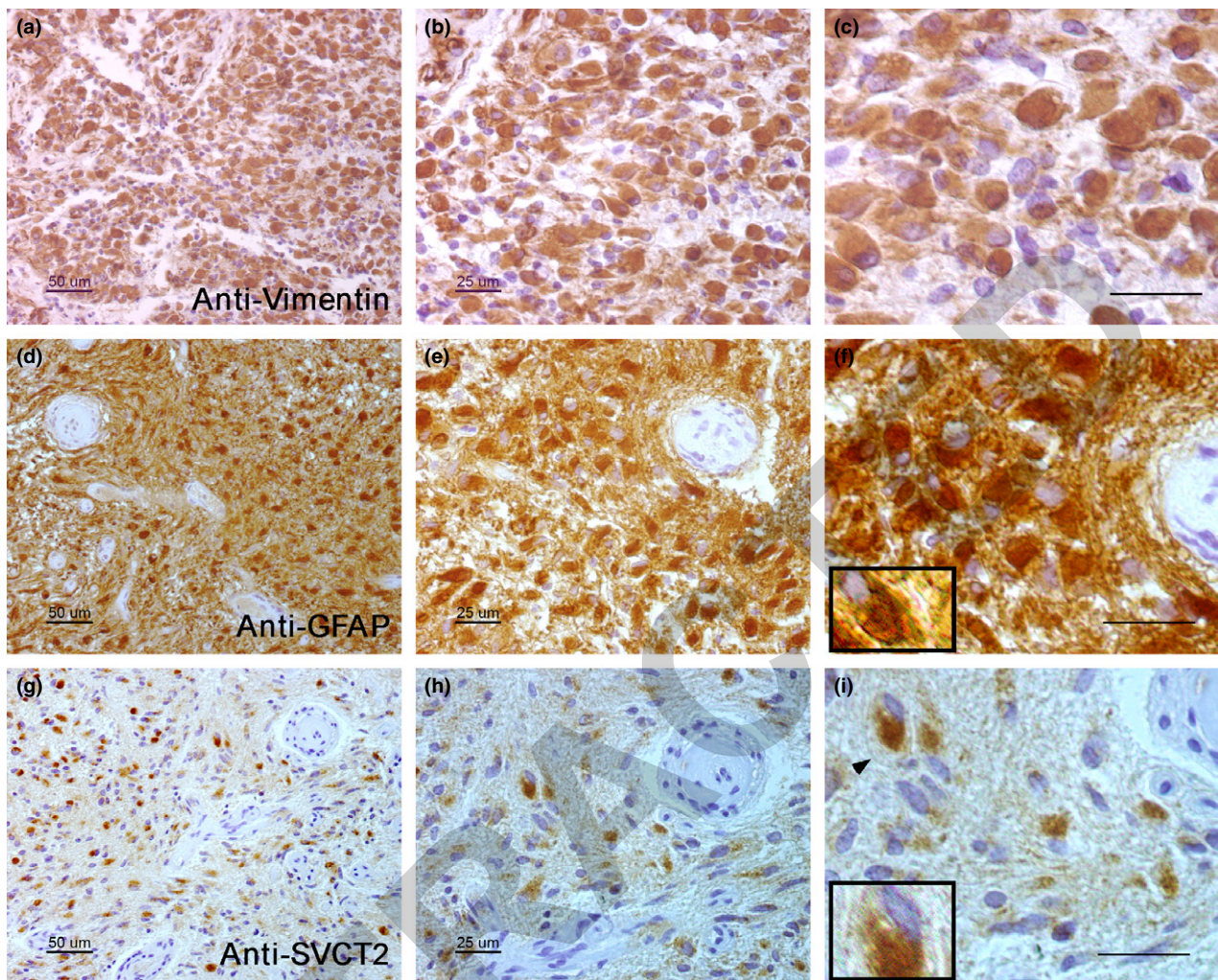


**Fig. 3** *In situ* immunolocalization of sodium-vitamin C co-transporter isoform 2 (SVCT2) in human glioblastoma multiforme. Histological sections (7  $\mu\text{m}$ ) obtained from human paraffin embedded Glioblastoma multiforme (GBM) tissues fixed in 10% formalin were immunoprobed with glioma markers and anti-SVCT2. (a–f) Immunodetection of tumor

cells with anti-vimentin and anti-gliofibrillary acid protein (d–f) antibodies. (g–i) Intracellular SVCT2 immunoreaction in glioma cells. Insets show magnified details, and arrow head indicates the cell limit (i). Scale bars, 50  $\mu\text{m}$  (a, d, g) and 25  $\mu\text{m}$  (b, c, e, f, h, i). Data are representative of at least six human GBM samples.

indicated high levels of intracellular SVCT2 expression in tumor cells, which was not observed at the cell membrane (Fig. 3g–i; i, arrow head), confirming SVCT2 expression and intracellular localization *in situ*.

#### Human glioma cells show high levels of 2-DOG and DHA uptake capacity

Tumor cells express high levels of GLUTs that support high glucose uptake and metabolism, some of which also transport DHA (Spielholz *et al.* 1997). Thus, kinetic analysis for 2-DOG and DHA uptake in TC620 cells was undertaken. High-level uptake of 2-DOG was observed at concentrations ranging from 0.2–20 mM, reaching the half equilibrium concentration in less than 1 min (Fig. 4a). 2-DOG uptake revealed two slopes; the first linear uptake represents the

initial velocity, and the latter is influenced by non-phosphorylated 2-DOG accumulation and efflux generated by decreased hexokinase activity because of ATP-depletion. To prevent miscalculation of transport kinetic parameters during this second phase, we performed the analyses at 30 s, a period in which all concentrations were in the initial velocity phase (Fig. 4a). Uptake of 2-DOG was sodium-insensitive as revealed when replacing sodium with choline (Fig. 4b). Furthermore, a saturation plot using 0.05–20 mM 2-DOG showed a typical Michaelian curve and initial saturation approximately at 2 mM 2-DOG (Fig. 4c). A double reciprocal plot revealed a single functional component for 2-DOG uptake with a  $K_m$  of 4 mM and a  $V_{max}$  of 7  $\text{nmol} \times 10^6$  cells/min (Fig. 4c; inset). A semi-log plot for cytochalasin B (Cyt B)-dependent inhibition of 0.2 mM

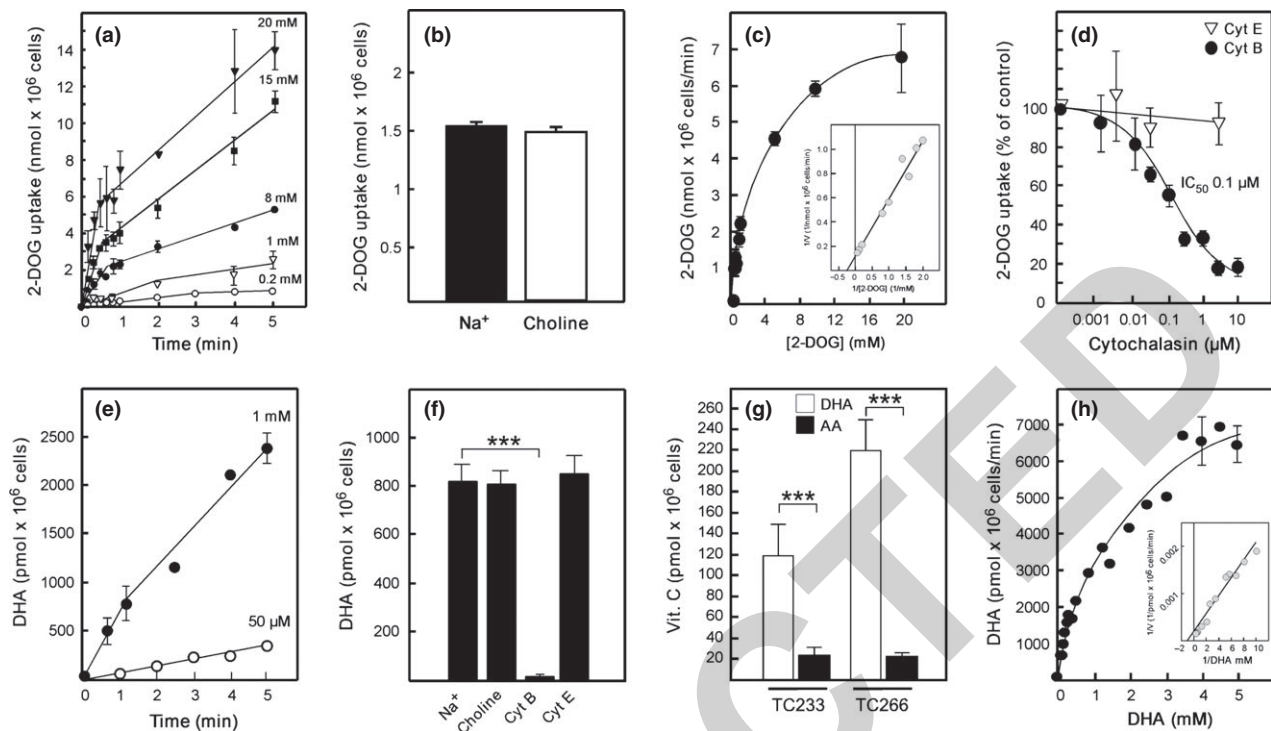


**Fig. 4** Kinetic analysis of facilitative hexose transporters. TC620 cells were assayed for radiolabeled 2-deoxy-D-glucose (2-DOG) and DHA uptake. (a) Time course of 0.2–20 mM 2-DOG uptake. (b) Uptake of 0.2 mM 2-DOG at 5 min replacing 135 mM NaCl with 135 mM choline chloride. (c) Saturation curve for 0.5–20 mM 2-DOG uptake at 30 s; Inset, Lineweaver–Burk transformation. (d) Inhibition semi-log plot for 2-DOG uptake inhibition by Cyt B. (e) Time course for 0.05 mM and 1 mM DHA uptake up to 5 min. (f) Controls for facilitative hexose transporter (GLUT)-specific uptake of 50  $\mu$ M DHA at 15 min with

2-DOG uptake at 2 min showed a half-maximal inhibition concentration ( $IC_{50}$ ) of 0.1  $\mu$ M, which was similar to previous reports (Garcia *et al.* 2003; Hresko and Hruz 2011). However, 2-DOG uptake was not inhibited by cytochalasin E, used as negative control (Fig. 4d).

The capacity of glioma cells for DHA uptake was next evaluated. Time-course uptake assays up to 5 min using 0.05 and 1 mM DHA showed high DHA uptake at similar levels to 2-DOG (Fig. 4e) and much higher than that observed for AA uptake. As DHA uptake after 1 min showed a shift in the slope using the highest concentration (Fig. 4e), we measured uptake at 30 s (i.e., the initial velocity phase) throughout the kinetic parameter analysis. Uptake of DHA was independent of sodium ions but greatly inhibited by Cyt B (Fig. 4f). Furthermore, uptake assays performed with cells isolated from human glioma biopsies TC233 (grade III) and TC236 (grade IV) showed similar DHA uptake capacity, which was 6- to 10-fold higher than AA uptake (Fig. 4g). Dose response assays with TC620 cells using 0.125–5 mM DHA at 30 s showed a Michaelian curve (Fig. 4h), and double-reciprocal analysis showed a single functional component with a  $K_m$  of

135 mM NaCl, 135 mM choline chloride, 30  $\mu$ M Cyt B or the non-GLUT-specific cytochalasin E. (g) 100  $\mu$ M DHA uptake in TC233 (grade III) and TC236 (grade IV) glioma cultures from human biopsies at 1 min. (h) Saturation plot for 0.1–5 mM DHA uptake at 30 s in TC620 cells. Inset, Double reciprocal plot. Kinetic assays were performed at 22°C unless otherwise indicated. Data represent means  $\pm$  SD of three independent experiments. \*\*\* $p > 0.001$ , Student's unpaired *t*-test.

0.8 mM and a  $V_{max}$  of 6.8  $\text{nmol} \times 10^6 \text{ cells}/\text{min}$  (Fig. 4h; inset). Together these functional data indicate high levels of glucose and DHA uptake in glioma cells with kinetic parameters that signify the presence of functional GLUT1.

#### High glucose and DHA uptake by glioma cells through GLUT1

To better define GLUT isoform expression in glioma, RT-PCR analysis using cDNA obtained from total RNA extracts of TC620 glioma cells and specific primers for the classical GLUTs (GLUT1–5) was undertaken. As shown in Fig. 5a, only GLUT1 mRNA expression was observed. Western blot analysis of total protein extracts from TC620 cells and rat brain (positive control) showed a broad protein band of 45 kDa (Fig. 5b) that was detected in rat brain and co-migrated with the glioma samples (lanes 1 and 2). Negative controls without primary antibody incubation showed no immunoreaction (Fig. 5b; lanes 3 and 4). Confocal microscopy using 3D-rendering analysis of GLUT-1 immunoreactivity in TC620 cells showed high intracellular and cell membrane GLUT1 labeling (Fig. 5c–h).

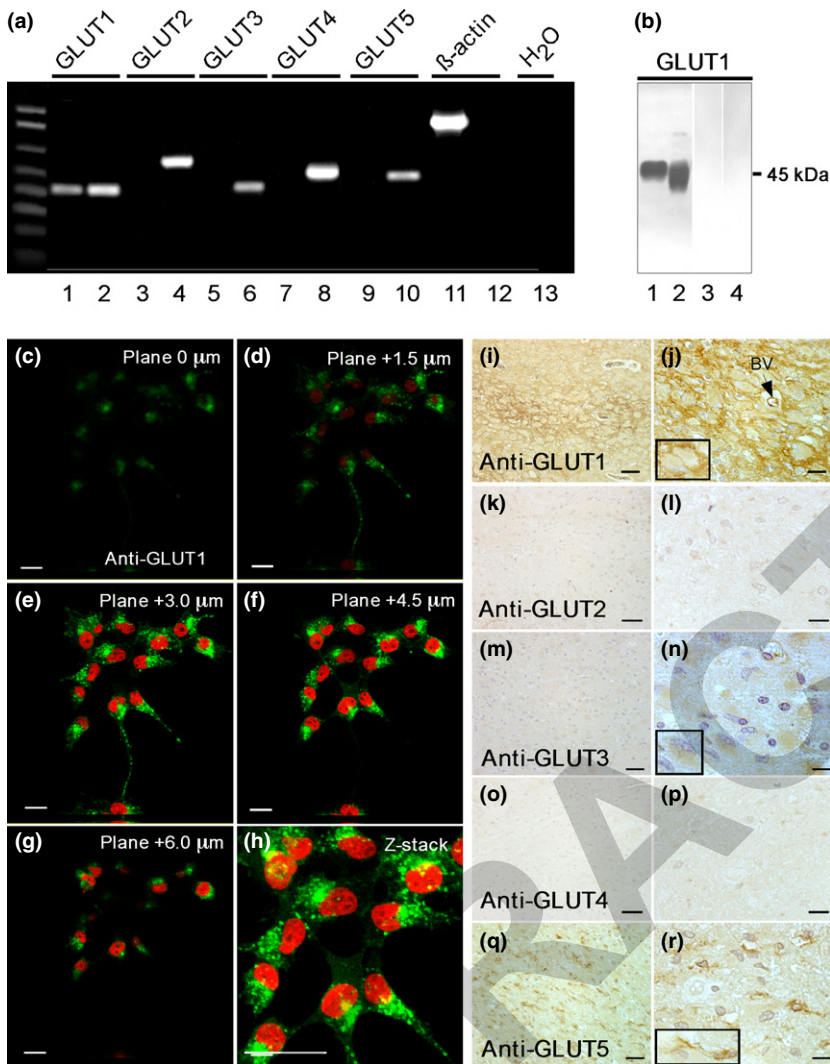


**Fig. 5** Analysis of facilitative hexose transporter (GLUT) expression in human glioma. (a) RT-PCR using specific primers for GLUTs 1-5 (lanes 1, 3, 5, 7, and 9); positive controls consisted of plasmidial GLUT 1-5 human sequences (lanes 2, 4, 6, 8, and 10) and housekeeping reaction for  $\beta$ -actin (lane 11). Negative controls were RT- (lane 12) and reaction without cDNA (lane 13). (b) Western blot analysis for GLUT1 protein expression in TC620 cell samples (lane 2), and whole rat brain (lane 1) was used as positive control. Omission of primary antibody was used as negative controls (lanes 4 and 3, respectively). (c-h) Confocal 3D-rendering analysis of GLUT1 immunolocalization (green) with propidium iodine nuclear stain in TC620 cells. (i-r) *In situ* bright field immunolocalization of GLUT1-5 in human glioblastoma multiforme biopsies using peroxidase-3,3'-diaminobenzidine immunoreaction (brown). Insets, higher magnification of cells. BV indicates blood vessels. Scale bars, 100  $\mu$ m (i, k, m, o, q), 50  $\mu$ m (c-h) and 25  $\mu$ m (j, l, n, p, r).

In addition, immunolocalization in human GBM tissues confirmed high GLUT1 expression in cells with tumor morphology and blood vessels (Fig. 5i and j). Furthermore, lower levels of GLUT3 expression were also observed (Fig. 5m and n), and GLUT5 immunoreaction was detected in ramified cells with small nuclei and defined as tumor-associated microglia (Fig. 5q and r). Neither GLUT2 nor GLUT4 was detected in GBM biopsies (Fig. 5k, l and o, p, respectively). In addition to the analyses performed with TC620 cells, we confirmed most of the results using human GBM U87 cells (Figure S1). U87 cells had low AA uptake capacity (Figure S1, Ia). Furthermore, like TC620 cells, U87 cells expressed the dnSVCT2 isoform (Figure S1, II), expressed proteins of the same molecular mass as detected by western blot analysis (Figure S1, IIIa) and displayed intracellular SVCT2 (Figure S1, IVc and d). Moreover, U87 cells expressed GLUT1 and GLUT3 (Figure S1, IIIc-f) with GLUT1 localization at the cell membrane (Figure S1, IVa and b). Furthermore, DHA uptake was 8-fold greater than

AA uptake (Figure S1, Ia and b). Together, these data indicate that glioma cells mainly depend on GLUT1 and possibly GLUT3 for vitamin C uptake and accumulation.

#### The Bystander effect allows effective vitamin C uptake in glioma cells

We have previously reported a mechanism for active generation of stromal DHA called the Bystander effect, which is a model for loading a peripheral tumor with vitamin C (Nualart *et al.* 2003). To determine if the Bystander effect could increase tumor vitamin C loading, microglial and human glioma TC620 cells were employed. Because of the high number of microglial cells required for Bystander uptake assays and the complexity of their isolation, cultured HL60 cells, which have a common origin with microglia (Chan *et al.* 2007), were used as a microglial model. After adherent TC620 cells were incubated with a HL60 cell suspension in the presence of <sup>14</sup>C-AA and PMA, a NADPH-oxidase activator (Fig. 6i), superoxide generation by HL60

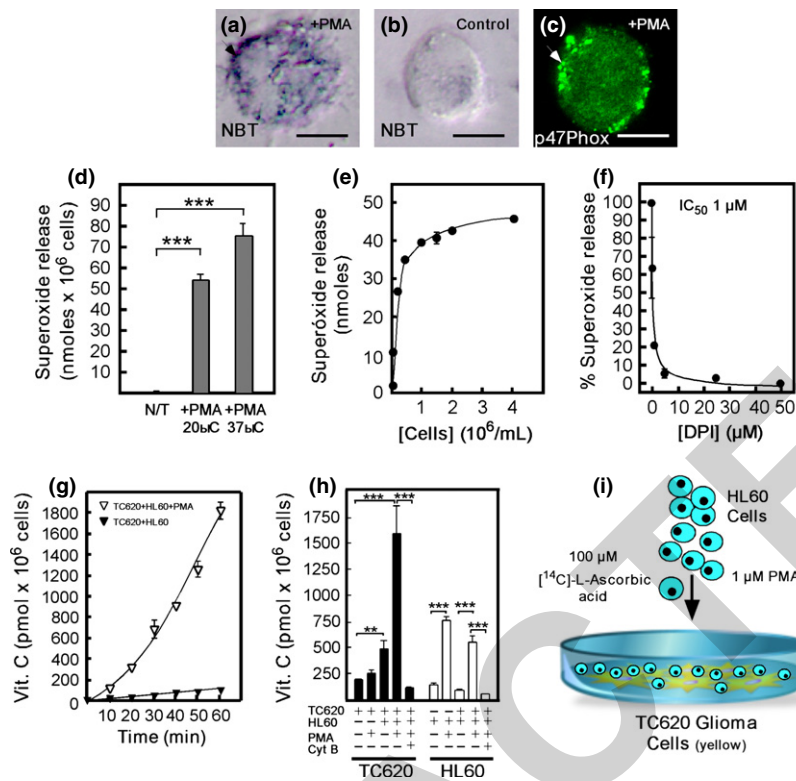


**Fig. 6** *In vitro* Bystander effect between human myeloid HL60 and glioma TC620 cells. Cultured HL60 cells were analyzed for superoxide generation and viability for the Bystander effect. (a and b) Intracellular nitro blue tetrazolium (NBT) reduction in HL60 cells treated with 1  $\mu$ M phorbol-12-myristate-13-acetate (PMA) (a) or dimethylsulfoxide (b). (c) Immunolocalization of NADPH-oxidase p47Phox subunit (green) in HL60 cells treated 1 h with 1  $\mu$ M PMA. Arrows indicate cell limit. (d), Cytochrome *c* superoxide liberation assay at 2 h in 1  $\mu$ M PMA-activated HL60 cells indicating temperature dependence. (e) Effect of HL60 cell density on superoxide release at 1 h. (f) Dose-dependence

curve for diphenylene iodonium (DPI) inhibition of superoxide release showing an  $IC_{50}$  of 1  $\mu$ M. (g) Bystander effect between co-incubated HL60 and TC620 cells, showing time course of vitamin C uptake in TC620 cells in the absence (filled triangles) or presence (white triangles) of 1  $\mu$ M PMA. (h) Bystander uptake of vitamin C in TC620 and HL60 cells indicated separately. (i) Diagram showing the Bystander effect experimental settings. Data represent means  $\pm$  SD of three independent experiments. \*\* $p > 0.01$ , \*\*\* $p > 0.001$ , Student's unpaired *t*-test. Scale bars, 10  $\mu$ m.

cells was assessed using the NBT assay that detects intracellular oxidants. Activation with 1  $\mu$ M PMA after 1 h generated a dense formazan deposition at the cell membrane that was not observed when incubated with dimethylsulfoxide (Fig. 6a and b, respectively). Similarly, the NADPH-oxidase subunit, p47Phox, had similar distribution as observed by the formazan deposits (Fig. 6c). The cytochrome *c* reduction assay revealed high superoxide liberation that was temperature-sensitive, decreasing by 27% at 20°C compared to 37°C (Fig. 6d). Furthermore, a limited increase in superoxide generation beyond  $0.5 \times 10^6$  cells/mL was observed, reaching a plateau of approximately 45 nmol superoxide/ $1 \times 10^6$  cells/h (Fig. 6e). Superoxide production was effectively inhibited by increasing concentrations of the NADPH-oxidase inhibitor, DPI, observing an  $IC_{50}$  of 1  $\mu$ M and a 92% inhibition at 5  $\mu$ M DPI (Fig. 6f). Furthermore, uptake of vitamin C in adherent cultures of TC620 cells incubated with HL60 cells in suspension and 50  $\mu$ M

radiolabeled AA showed low uptake levels ( $< 100$  pmol  $\times 10^6$  cells) up to 60 min (Fig. 6g; black triangles). However, after addition of 1  $\mu$ M PMA to the co-cultures, vitamin C uptake increased more than 18-fold at 60 min (Fig. 6g; white triangles), which was inhibited by 92% with 30  $\mu$ M Cyt B, indicating DHA uptake through GLUT1 (Fig. 6h). Although these results indicate the efficiency of the Bystander effect in promoting DHA uptake by glioma cells, HL60 cells competed for approximately 1/3 of the generated DHA.

## Discussion

Malignant gliomas are among the most devastating and untreatable cancers. Despite therapy-related progress for other types of cancers, the life expectancy of glioma patients has not increased significantly during the past half century due at least in part to the tumor's resistance to oxidative

damage (Bao *et al.* 2006). AA, the reduced form of vitamin C, is one of the most important scavengers of ROS in the CNS, and its uptake through SVCT2 has been characterized in normal CNS cells. This study determined the expression, localization, and function of SVCT2 and GLUTs to define the preferential mechanism of vitamin C uptake in cultured human glioma cells and GBM tissues. The low AA uptake rates coupled with the intracellular localization of SVCT2 indicated that accumulation of vitamin C by this mechanism was not possible. In addition, high 2-DOG uptake through GLUT1, which also permitted uptake of high levels of DHA, was observed. Furthermore, uptake of large levels of vitamin C by glioma cells was observed upon oxidation of extracellular AA to DHA through the Bystander effect. Finally, the role of microglial oxidative burst in modulating vitamin C availability in glioma microenvironment was evaluated.

In this study, immunocytochemical analysis of glioma cells revealed high levels of SVCT2 expression both in cultured TC620 human glioma cells and human GBM tissues. However, SVCT2 was primarily localized within the intracellular compartment, co-localizing mainly with the Golgi apparatus and endoplasmic reticulum markers, GBF-1 and calnexin, respectively. Previously, a short SVCT2 mRNA isoform, lacking 342 bp, was cloned from human fetal brain; this isoform inhibited AA uptake in a dominant-negative fashion when over-expressed (Lutsenko *et al.* 2004). Although different molecular weights have been reported for SVCT2 in the literature, the predicted molecular mass is around 70 kDa for the full length isoform. In addition, phosphorylation and glycosylation would increase the molecular weight by an additional 5–10 kDa. On the other hand, little is known about the dnSVCT2 in human samples. Lutsenko *et al.* (2004) showed an abnormally heavy 70 kDa band when over-expressed as a His-tagged recombinant protein. However, many His-tagged proteins show abnormal migration in sodium dodecyl sulfate–polyacrylamide gel electrophoresis. In this article, the expression of glioma cells SVCT2 isoforms was detected using western blot analysis. A small polypeptide with a molecular mass of 50 kDa was detected, which was similar to the 55 kDa dnSVCT2 isoform cloned previously (Wu *et al.* 2007). Thus, the expression of this short isoform in glioma cells could be responsible for the intracellular localization of SVCT2. Similarly, a SVCT2-positive band of 130 kDa was observed in glioma samples, which could represent a hetero-oligomer of the 50 kDa and 75 kDa isoforms. Supporting this finding, several reports have shown that the cellular localization of membrane proteins can be regulated by dominant-negative proteins or SDS-resistant oligomerization (Galbiati *et al.* 1999; Haugeo *et al.* 1996; Hong *et al.* 2005; Kilic and Rudnick 2000; Sarmiento *et al.* 2004).

As with most tumor cells, glioma cells undergo metabolic transformations that lead to increased glucose uptake through up-regulation of glycolytic enzymes and glucose transporter

expression (Mangiardi and Yodice 1990). In this study, TC620 cells had an elevated capacity for 2-DOG uptake. Because this 2-DOG uptake was sodium-independent, transport was not through sodium-dependent glucose transporters. Furthermore, GLUT specificity was confirmed using the classic inhibitor, Cyt B (Deves and Krupka 1978), and determination of 2-DOG kinetic parameters. In addition, strong immunolabeling of GLUT1 in cultured TC620 cells and in human GBM tissues was observed, which also transported DHA with high affinity.

Tumoricidal effects of AA have been observed in glioblastoma xenografts that were subjected to parenteral administration of pharmacological doses of ascorbate (Chen *et al.* 2007). The authors reported that hydrogen peroxide was produced in the tumoral milieu when AA reacted with extracellular metalloproteases and oxygen, thereby inducing cell damage that concluded in evident tumor cell death (Chen *et al.* 2007). Thus, the effect of AA on different tumor types could be highly dependent on its histological context. In the brain, glioblastoma tumors are highly infiltrated with microglia; thus, the final effect of AA could be different from that observed in peripheral xenograft tumors treated with parenteral ascorbate administration.

We have previously proposed that peripheral tumors, which are unable to capture AA, could increase their vitamin C uptake by oxidizing stromal AA to DHA by superoxide-releasing infiltrating neutrophils through the oxidative burst, called the Bystander effect (Nualart *et al.* 2003). Similarly, several studies using rodent glioma models and human biopsies showed that gliomas can be comprised of up to 45% of microglial cells in their microenvironment (Morantz *et al.* 1979; Nishie *et al.* 1999; Seyfried 2001; Shinonaga *et al.* 1988), because of chemotaxis induced by glioma-secreted chemokines, including MCP-1, and vascular leakage (Nakamura 2002; Nimmerjahn *et al.* 2005). Like neutrophils, activated microglia, can produce extracellular superoxide (Dheen *et al.* 2007; Sankarapandi *et al.* 1998). We propose that the increase in microglial cell density with malignant progression of gliomas may produce an oxidizing microenvironment for AA oxidation, similar to the Bystander effect. This is supported by data from this study in which glioma cells captured DHA at rates 8-fold higher than that observed for AA uptake. In addition, DHA kinetic assays showed sodium independence, Cyt B inhibition and kinetic parameters concordant with GLUT1 functionality (Rumsey *et al.* 1997). Our findings are further supported by the *in situ* detection of GLUT1 expression as the main DHA transporter in human GBM tissues and by human GBM cell culture uptake assays that confirmed a 7-fold DHA uptake preference over AA. U87 GBM cells with astroglial characteristics expressed GLUT3; however, our *in situ* data revealed no clear membrane localization as observed for GLUT1. Overall, glioma cells showed molecular features indicating a vitamin C accumulation system dependent on DHA availability.

In this study, the influence of the Bystander effect on glioma cells was undertaken using HL60 cells as a superoxide-releasing microglia cell model because of the complexity of isolation and high number of microglial cells needed for uptake assays. As we had previously defined with peripheral tumor cells (Nualart *et al.* 2003), the Bystander effect induced a staggering 18-fold increase in vitamin C uptake by glioma cells after 1 h co-incubation with activated HL60 cells.

In conclusion, the data from this study indicate that like other tumor cells, human glioma cells are poorly able to accumulate vitamin C in the form of AA (Fig. 7), which could be related to the intracellular localization of SVCT2 and the expression of dnSVCT2. However, unlike most tumors, the histological context of gliomas and the presence of a cellular partner, namely microglia, give high-grade gliomas an additional option for vitamin C uptake that depends on microglial activation and superoxide release. In this context, the close contact between glioma and activated microglial cells (Fig. 7) could induce the Bystander effect, oxidizing extracellular AA to DHA, which can be captured by glioma cells through GLUT1. Subsequent intracellular reduction of DHA would prevent DHA efflux through bi-directional GLUT1, thereby loading glioma cells with high levels of AA, which may induce resistance to cytostatic therapies and/or support glioma growth.

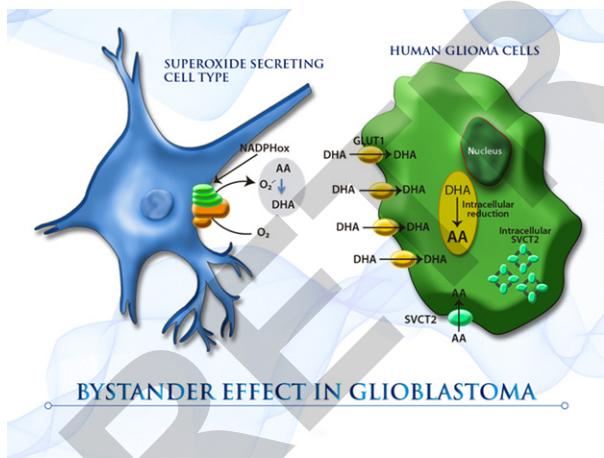


**Fig. 7** Bystander uptake mechanism in human gliomas. Human glioma cells are unable to capture elevated levels of ascorbic acid (AA) because of intracellular localization of sodium-vitamin C cotransporter isoform 2; however, increased expression of facilitative hexose transporter1 enables glioma cells to capture DHA if present. Active generation of DHA could be possible in high-grade gliomas because of the high infiltration of microglial cells (up to 45%). Microglial-mediated Bystander effect, as shown with HL60 cells, could allow extracellular generation of DHA through NADPH-oxidase superoxide liberation and oxidation of stromal AA to DHA. Intracellular enzymatic reduction of DHA to AA would then allow for scavenging of therapy-induced reactive oxygen species, preventing cellular damage and/or death.

## Acknowledgements

This study was supported by FONDECYT grant #1100396 (to FN) and a CONICYT-PIA ECM-12 grant (to FN). The funders had no role in study design, data collection and analysis, decision to publish, or preparation of the manuscript. No potential conflicts of interest were disclosed.

## Supporting information

Additional supporting information may be found in the online version of this article at the publisher's web-site:

**Figure S1.** Expression of vitamin C transporters in human U-87 glioblastoma cells.

## References

- Angelow S., Haselbach M. and Galla H. J. (2003) Functional characterisation of the active ascorbic acid transport into cerebrospinal fluid using primary cultured choroid plexus cells. *Brain Res.* **988**, 105–113.
- Astuya A., Caprile T., Castro M., *et al.* (2005) Vitamin C uptake and recycling among normal and tumor cells from the central nervous system. *J. Neurosci. Res.* **79**, 146–156.
- Bao S., Wu Q., McLendon R. E., Hao Y., Shi Q., Hjelmeland A. B., Dewhirst M. W., Bigner D. D. and Rich J. N. (2006) Glioma stem cells promote radioresistance by preferential activation of the DNA damage response. *Nature* **444**, 756–760.
- Cameron E. and Pauling L. (1976) Supplemental ascorbate in the supportive treatment of cancer: Prolongation of survival times in terminal human cancer. *Proc. Natl Acad. Sci. USA* **73**, 3685–3689.
- Cameron E. and Pauling L. (1978) Supplemental ascorbate in the supportive treatment of cancer: reevaluation of prolongation of survival times in terminal human cancer. *Proc. Natl Acad. Sci. USA* **75**, 4538–4542.
- Chan W. Y., Kohsaka S. and Rezaie P. (2007) The origin and cell lineage of microglia: new concepts. *Brain Res. Rev.* **53**, 344–354.
- Chen Q., Espey M. G., Sun A. Y. *et al.* (2007) Ascorbate in pharmacologic concentrations selectively generates ascorbate radical and hydrogen peroxide in extracellular fluid in vivo. *Proc Natl Acad Sci U S A.* **104**, 8749–8754.
- Deves R. and Krupka R. M. (1978) Cytochalasin B and the kinetics of inhibition of biological transport: a case of asymmetric binding to the glucose carrier. *Biochim. Biophys. Acta* **510**, 339–348.
- Dheen S. T., Kaur C. and Ling E. A. (2007) Microglial activation and its implications in the brain diseases. *Curr. Med. Chem.* **14**, 1189–1197.
- Dohrmann G. J., Farwell J. R. and Flannery J. T. (1976) Glioblastoma multiforme in children. *J. Neurosurg.* **44**, 442–448.
- Galbiati F., Volonte D., Minetti C., Chu J. B. and Lisanti M. P. (1999) Phenotypic behavior of caveolin-3 mutations that cause autosomal dominant limb girdle muscular dystrophy (LGMD-1C). Retention of LGMD-1C caveolin-3 mutants within the golgi complex. *J. Biol. Chem.* **274**, 25632–25641.
- Garcia Mde L., Salazar K., Millan C., *et al.* (2005) Sodium vitamin C cotransporter SVCT2 is expressed in hypothalamic glial cells. *Glia* **50**, 32–47.
- Garcia M. A., Millan C., Balmaceda-Aguilera C., *et al.* (2003) Hypothalamic ependymal-glial cells express the glucose transporter GLUT2, a protein involved in glucose sensing. *J. Neurochem.* **86**, 709–724.

- Godoy A., Ulloa V., Rodríguez F., *et al.* (2006) Differential subcellular distribution of glucose transporters GLUT1-6 and GLUT9 in human cancer: ultrastructural localization of GLUT1 and GLUT5 in breast tumor tissues. *J. Cell. Physiol.* **207**, 614–627.
- Guaiquil V. H., Farber C. M., Golde D. W. and Vera J. C. (1997) Efficient transport and accumulation of vitamin C in HL-60 cells depleted of glutathione. *J. Biol. Chem.* **272**, 9915–9921.
- Haugeto O., Ullensvang K., Levy L. M., Chaudhry F. A., Honore T., Nielsen M., Lehre K. P. and Danbolt N. C. (1996) Brain glutamate transporter proteins form homomultimers. *J. Biol. Chem.* **271**, 27715–27722.
- Heaney M. L., Gardner J. R., Karasavvas N., Golde D. W., Scheinberg D. A., Smith E. A. and O'Connor O. A. (2008) Vitamin C antagonizes the cytotoxic effects of antineoplastic drugs. *Cancer Res.* **68**, 8031–8038.
- Hong M., Xu W., Yoshida T., Tanaka K., Wolff D. J., Zhou F., Inouye M. and You G. (2005) Human organic anion transporter hOAT1 forms homooligomers. *J. Biol. Chem.* **280**, 32285–32290.
- Hresko R. C. and Hruz P. W. (2011) HIV protease inhibitors act as competitive inhibitors of the cytoplasmic glucose binding site of GLUTs with differing affinities for GLUT1 and GLUT4. *PLoS ONE* **6**, e25237.
- Kilic F. and Rudnick G. (2000) Oligomerization of serotonin transporter and its functional consequences. *Proc. Natl Acad. Sci. USA* **97**, 3106–3111.
- Liang W. J., Johnson D. and Jarvis S. M. (2001) Vitamin C transport systems of mammalian cells. *Mol. Membr. Biol.* **18**, 87–95.
- Linster C. L. and Van Schaftingen E. (2007) Vitamin C. Biosynthesis, recycling and degradation in mammals. *FEBS J.* **274**, 1–22.
- Louis D. N., Ohgaki H., Wiestler O. D., Cavenee W. K., Burger P. C., Jouvet A., Scheithauer B. W. and Kleihues P. (2007) The 2007 WHO classification of tumours of the central nervous system. *Acta Neuropathol.* **114**, 97–109.
- Lutsenko E. A., Carcamo J. M. and Golde D. W. (2004) A human sodium-dependent vitamin C transporter 2 isoform acts as a dominant-negative inhibitor of ascorbic acid transport. *Mol. Cell. Biol.* **24**, 3150–3156.
- Mangiardi J. R. and Yodice P. (1990) Metabolism of the malignant astrocytoma. *Neurosurgery* **26**, 1–19.
- Manuelidis L., Yu R. K. and Manuelidis E. E. (1977) Ganglioside content and pattern in human gliomas in culture. Correlation of morphological changes with altered gangliosides. *Acta Neuropathol.* **38**, 129–135.
- Mendiratta S., Qu Z. C. and May J. M. (1998) Enzyme-dependent ascorbate recycling in human erythrocytes: role of thioredoxin reductase. *Free Radic Biol Med* **25**, 221–228.
- Millan C., Martinez F., Cortes-Campos C., *et al.* (2010) Glial glucokinase expression in adult and post-natal development of the hypothalamic region. *ASN Neuro* **2**, e00035.
- Moertel C. G., Fleming T. R., Creagan E. T., Rubin J., O'Connell M. J. and Ames M. M. (1985) High-dose vitamin C versus placebo in the treatment of patients with advanced cancer who have had no prior chemotherapy. A randomized double-blind comparison. *N. Engl. J. Med.* **312**, 137–141.
- Morantz R. A., Wood G. W., Foster M., Clark M. and Gollahon K. (1979) Macrophages in experimental and human brain tumors. Part 2: studies of the macrophage content of human brain tumors. *J. Neurosurg.* **50**, 305–311.
- Nakamura Y. (2002) Regulating factors for microglial activation. *Biol. Pharm. Bull.* **25**, 945–953.
- Nimmerjahn A., Kirchhoff F. and Helmchen F. (2005) Resting microglial cells are highly dynamic surveillants of brain parenchyma in vivo. *Science* **308**, 1314–1318.
- Nishie A., Ono M., Shono T., *et al.* (1999) Macrophage infiltration and heme oxygenase-1 expression correlate with angiogenesis in human gliomas. *Clin. Cancer Res.* **5**, 1107–1113.
- Nualart F. J., Rivas C. I., Montecinos V. P., Godoy A. S., Guaiquil V. H., Golde D. W. and Vera J. C. (2003) Recycling of vitamin C by a bystander effect. *J. Biol. Chem.* **278**, 10128–10133.
- Nualart F., Castro T., Low M., *et al.* (2012a) Dynamic expression of the sodium-vitamin C co-transporters, SVCT1 and SVCT2, during perinatal kidney development. *Histochem. Cell Biol.* **139**, 233–247.
- Nualart F., Salazar K., Oyarce K., *et al.* (2012b) Typical and atypical stem cells in the brain, vitamin C effect and neuropathology. *Biol. Res.* **45**, 243–256.
- Ohgaki H. and Kleihues P. (2005) Epidemiology and etiology of gliomas. *Acta Neuropathol.* **109**, 93–108.
- Rice M. E. (2000) Ascorbate regulation and its neuroprotective role in the brain. *Trends Neurosci.* **23**, 209–216.
- Rumsey S. C., Kwon O., Xu G. W., Burant C. F., Simpson I. and Levine M. (1997) Glucose transporter isoforms GLUT1 and GLUT3 transport dehydroascorbic acid. *J. Biol. Chem.* **272**, 18982–18989.
- Sankarapandi S., Zweier J. L., Mukherjee G., Quinn M. T. and Huso D. L. (1998) Measurement and characterization of superoxide generation in microglial cells: evidence for an NADPH oxidase-dependent pathway. *Arch. Biochem. Biophys.* **353**, 312–321.
- Sarmiento J. M., Anazco C. C., Campos D. M., Prado G. N., Navarro J. and Gonzalez C. B. (2004) Novel down-regulatory mechanism of the surface expression of the vasopressin V2 receptor by an alternative splice receptor variant. *J. Biol. Chem.* **279**, 47017–47023.
- Savini I., Rossi A., Pierro C., Avigliano L. and Catani M. V. (2008) SVCT1 and SVCT2: key proteins for vitamin C uptake. *Amino Acids* **34**, 347–355.
- Schiffner D., Manazza A. and Tamagno I. (2006) Nestin expression in neuroepithelial tumors. *Neurosci. Lett.* **400**, 80–85.
- Seyfried T. N. (2001) Perspectives on brain tumor formation involving macrophages, glia, and neural stem cells. *Perspect. Biol. Med.* **44**, 263–282.
- Shinoga M., Chang C. C., Suzuki N., Sato M. and Kuwabara T. (1988) Immunohistological evaluation of macrophage infiltrates in brain tumors. *Correlation with peritumoral edema. J Neurosurg* **68**, 259–265.
- Spielholz C., Golde D. W., Houghton A. N., Nualart F. and Vera J. C. (1997) Increased facilitated transport of dehydroascorbic acid without changes in sodium-dependent ascorbate transport in human melanoma cells. *Cancer Res.* **57**, 2529–2537.
- Sudo S., Tanaka J., Toku K., Desaki J., Matsuda S., Arai T., Sakanaka M. and Maeda N. (1998) Neurons induce the activation of microglial cells in vitro. *Exp. Neurol.* **154**, 499–510.
- Telang S., Clem A. L., Eaton J. W. and Chesney J. (2007) Depletion of ascorbic acid restricts angiogenesis and retards tumor growth in a mouse model. *Neoplasia* **9**, 47–56.
- Watkins S. and Sontheimer H. (2012) Unique biology of gliomas: challenges and opportunities. *Trends Neurosci.* **35**, 546–556.
- Wen P. Y. and Kesari S. (2008) Malignant gliomas in adults. *N. Engl. J. Med.* **359**, 492–507.
- Wu X., Zeng L. H., Taniguchi T. and Xie Q. M. (2007) Activation of PKA and phosphorylation of sodium-dependent vitamin C transporter 2 by prostaglandin E2 promote osteoblast-like differentiation in MC3T3-E1 cells. *Cell Death Differ.* **14**, 1792–1801.
- Yi L., Xiao H., Xu M., *et al.* (2011) Glioma-initiating cells: a predominant role in microglia/macrophages tropism to glioma. *J. Neuroimmunol.* **232**, 75–82.
- Zhai H., Heppner F. L. and Tsirka S. E. (2011) Microglia/macrophages promote glioma progression. *Glia* **59**, 472–485.